Low-Symmetry Structures of Au_{32}^{Z} ($Z = +1, 0, -1$) Clusters

Abraham F. Jalbout,[†] Flavio F. Contreras-Torres,[†] Luis A. Pérez,[‡] and Ignacio L. Garzón*[,‡]

Instituto de Química, Universidad Nacional Autónoma de México, México D.F., México, and Instituto de Física, Universidad Nacional Autónoma de México, Apartado Postal 20-364, 01000 México D.F, México

Received: June 21, 2007; In Final Form: September 19, 2007

In this work, we have explored new stable structures of the Au_{32}^{Z} ($Z = +1, 0, -1$) clusters. Theoretical calculations using density functional theory within the generalized-gradient approximation were performed. Our results show that, in the anion state (Au_{32}^{-}), low-symmetry (disordered) structures are preferred over the caged fullerene-like isomer. In addition, the cationic cluster (Au_{32}^{+}) also exhibits a disordered low-symmetry structure as its lowest energy configuration, but it is much closer in energy to the fullerene-like isomer. These results, obtained at $T = 0$ K, indicate that disordered structures for the Au_{32}^{-} and Au_{32}^{+} clusters may be detected not only at room temperature, as was experimentally verified for the Au_{32}^{-} one, but also at much lower temperatures.

Introduction

The study of gold clusters and related complexes is important because of their recent interest in nanotechnology.[1−6] Many interesting catalytic properties of supported and unsupported Au_n clusters have sparked more attention on the physical and chemical properties of systems of this type.[4,7] It is well-established that the strong relativistic effects of gold[8,9] cause the Au_n clusters to exhibit unique structures that isolate them from other metallic clusters. In recent investigations, it has been demonstrated that gold clusters (with $n < 12-14$) are commonly confined to two-dimensional structures;[10] however, the corresponding Cu and Ag clusters are three-dimensional.[11]

Among the most unusual properties of gold clusters was the prediction of a stable cagelike structure for the Au_{32} cluster. This cluster was found to have icosahedral (I_h) symmetry and has been referred to as the "golden fullerene", because of its similarity to C_{60}.[12,13] The stability induced for this system is related to what is known as spherical aromaticity.[12] The aromatic character of this cluster arises from the 32 6s electrons of gold, since the $2(N + 1)^2$ rule for spherical aromaticity is satisfied whereby $N = 3$. This type of structure is not predicted traditionally for metallic clusters, but it appears that aromaticity is related to the stability of the cagelike structure.[14] Attempts to synthesize and characterize such a structure have been proposed,[12,13] but to date, the formation of such a cluster is still uncertain.[15]

The direct experimental characterization of cluster structures is challenging, although electron diffraction studies have been shown to be a probable route for their elucidation.[16−18] Recent studies using trapped ion electron diffraction (TIED) in gold clusters have revealed interesting structural trends.[10,19] Other methods, such as photoelectron spectroscopy (PES),[15,20,21] combined with quantum mechanical calculations have been shown to be an adequate tool for determining physical properties of such clusters. PES[20] and TIED[10] have shown, for example, that the anionic Au_{20} cluster has a highly symmetric, tetrahedral structure, which has been confirmed to be the lowest energy configuration for this cluster.

On the theoretical side, the determination of the most stable structures of clusters is also challenging. It is well-known that the complexity of the potential energy surface increases dramatically with the cluster size, making it very difficult to locate the lowest-lying minima that correspond to stable cluster configurations. Additionally, the correct description of the cluster bonding requires quantum mechanical methods that are computationally time-consuming. Nevertheless, there has been theoretical evidence suggesting that the lowest energy structure for the Au_{32} cluster corresponds to cagelike geometry with I_h symmetry.[12,13,15] On the other hand, it has been theoretically shown that Au_n clusters may preferentially be nonsymmetric[22] or even chiral[23,24] for several values of n. However, this class of structures was not systematically considered in the most recent work performed on Au_{32}^{-}.[15] In the present theoretical study, we obtain that the most stable structures of Au_{32} are in fact nonsymmetric and disordered, for both the anionic and the cationic clusters. For the neutral cluster, the symmetric I_h structure is the most stable configuration, but as charges are added or taken away, its relative stability changes as well.

Moreover, we also show that the dicationic and dianionic states of Au_{32} cause structural distortions that result in modifications of the electron charge distributions, which could explain the relative differences in stabilities of the symmetric and disordered isomers of the charged Au_{32} clusters. The relative stability of the charged cluster isomers can again be discussed using the spherical aromaticity.[12] According to the $2(N + 1)^2$ rule, spherical aromaticity in Au_{32} clusters with $+1$ and $+2$ charges shall be destabilized as a result of weak aromatic effects. On the contrary, an increased number of electrons would need to be added or removed from the cluster for the above equation to be satisfied.

In this work, we report 10 low-symmetry isomers of the Au_{32} cluster in the cationic, anionic, and neutral states, which are found to be to be energetically stable. We also predict that, in the anionic and cationic states, they should be experimentally detected not only at room temperature, as was recently reported[15] for the anionic case, but also at much lower temperatures.

* To whom correspondance should be addressed. E-mail: garzon@fisica.unam.mx. Phone: +52-55-56225147. Fax: +52-55-56225015.
[†] Instituto de Química.
[‡] Instituto de Física.

10.1021/jp074852y CCC: $40.75 © 2008 American Chemical Society
Published on Web 01/01/2008

Computational Methods

The cluster structures presented herein were obtained following a procedure similar to that reported in previous publications by our group.[22−24] At the last stage of the calculations, the cluster structures were optimized by unconstrained relaxations using the forces calculated from density functional theory (DFT). The DFT calculations were performed with the SIESTA code,[25] using scalar relativistic norm-conserving pseudopotentials,[26] a double-ζ basis set,[11] and the generalized-gradient approximation (GGA) with the Perdew−Burke−Ernzerhof (PBE) parametrization.[27] This methodology has been used before to study the trends in the structure and bonding of noble metal clusters.[11,28] In particular, the energetics and structural and electronic properties of neutral and charged Au_n ($n = 2-13$) clusters, as well as the relative stability of the Au_{20} cluster, were studied using the same level of approximation as mentioned above,[11] obtaining good agreement with other theoretical studies and with experimental data, when they were available. Although we consider that the conclusions obtained in the above-mentioned study on smaller noble metal clusters[11] justify the use of the same methodology for the investigation of structural properties of neutral and charged Au_{32} clusters, it is important to mention that questions related to the use of other exchange-correlation functionals, spin-polarization calculations, or effects of a larger basis set have not been considered in the present work. Instead, a systematic search for the most stable configurations of neutral and charged Au_{32} clusters was attempted by performing local structural relaxations using DFT−GGA forces on the cluster geometries obtained from a global optimization procedure, combining genetic algorithms and a semiempirical many-body potential.[22−24]

Results and Discussion

From a previous theoretical study,[15] it was shown that the most stable isomer for Au_{32} is the I_h cagelike structure, which upon electron attachment undergoes a Jahn−Teller distortion to yield the D_{3d} structure for the Au_{32}^- cluster. While we obtain similar results for this particular anionic cluster isomer, we also found other low-symmetry, disordered isomers more stable than the D_{3d} isomer.

Figure 1 displays the optimized isomers of the Au_{32} cluster calculated as mentioned in the previous section. Only isomers **d** and **8** were found to be symmetric, which have I_h and C_{2v} symmetry, respectively. In the case of Au_{32}^- and Au_{32}^+, isomers **d** and **8** transform to D_{3d} and C_2 symmetry, respectively. Table 1 shows the relative energies (ΔE) in electronvolts of all isomers with respect to isomer **d**, as well as the highest occupied molecular orbital (HOMO)/lowest unoccupied molecular orbital (LUMO) gaps for the neutral case (denoted as GAP in Table 1). These results show that, for the cationic and anionic forms of Au_{32}, the low-symmetry (disordered) structures are favored over the **d** cagelike isomer, although for the cationic case the relative energy between isomers **d** and **10** is very small.

First, let us consider the **d** isomer of the neutral and charged states of the Au_{32} cluster. We have taken this isomer to be the reference point for the other structures and thereby assigned it a value of zero for its relative energy, for both the neutral and the charged clusters. As Table 1 shows, this isomer has a HOMO/LUMO gap of 1.53 eV for the neutral case. This value is significantly higher than the experimental value, but it is in agreement with the previously reported theoretical value also computed at the DFT−GGA level of theory.[15] Upon electron attachment and detachment, this structure undergoes a transformation to D_{3d} symmetry.

For isomer **1**, Table 1 shows that the total energy of the neutral and cationic species is higher with respect to the **d** structure as computed by DFT. On the other hand, electron attachment to the neutral cluster leads to an anion, which is lower in energy than the **d** isomer. This structure has no symmetry, and as we can see from Figure 1, it can be considered as a disordered cluster. From Table 1, it is shown that the HOMO/LUMO gap is 0.27 eV, which is very close to the experimental value of 0.30 eV, suggesting that it may be experimentally observed.

In the case of isomer **2**, we can see that it is higher in energy than **1** for the three charged states, as calculated using DFT method. Interestingly, the HOMO/LUMO gap is only about 0.03 eV, suggesting that it should be relatively reactive. The increased energy of this system will probably prevent its formation in an experimental environment. This structure is also disordered and does not have symmetry in any of the charge states studied in the present investigation.

For the neutral and cationic isomer **3**, we can see that there is a slight decrease in energy with respect to **2**. In the anionic state, it is more stable than the **d** isomer, and as stable as isomer **2**, but less stable in the cationic and neutral configurations than the caged hollow structure, which dominates in terms of stability. We have computed a HOMO/LUMO gap of 0.24 eV, which is close to the experimental value; however, as we will show later, there are other competing structures with closer values to the experimental result, and they have lower energy. These isomers are also disordered structures and do not have any internal symmetry.

The isomer **4** is also more stable than the **d** structure as an anion. For all structures reported in this work, this is a typical relationship, whereby the anions are all more stable than **d**, but for the neutral state, the **d** isomer dominates in terms of stability. The HOMO/LUMO gap is 0.09 eV, which is quite close to the value computed for species **2**, but isomer **4** is less energetically stable. Isomer **5** is less stable than **4**. Also, the HOMO/LUMO gap of species **5** is about 0.41 eV, but because of the fact that it is less stable, the structure may not be observed.

By considering the anionic isomers **6** and **7**, it is found that their relative energies with respect to the **d** isomer are −0.53 eV and −0.49 eV, respectively. In the cation state, it is found that **7** dominates over **6** in terms of stability at the DFT level of theory. We can note that up to now the structures under consideration lack symmetry in any of the states being studied (other than **d**, of course). It can also be readily observed that **7** has a HOMO/LUMO gap of 0.35 eV and **6** has one of 0.24 eV. While they are within the experimental error, we believe that their decreased stability relative to other cluster isomers will be an impediment for their formation.

In our potential energy surface scans, we found that isomer **8** has C_{2v} symmetry in the neutral state but then transforms to C_2 after electron attachment and detachment. This species forms a stable anion (with a ΔE of around −0.20 eV) and has physical properties similar to **4** (in terms of relative energy). Interestingly, this cluster has a HOMO/LUMO gap of around 0.40 eV, which is close to the experimental observations.[15]

Another isomer obtained from our search is **9**, which has a relative energy with respect to the **d** isomer of around −0.36 eV, for the anionic case, calculated at a DFT level. For isomer **9**, it is obtained that the HOMO/LUMO is around 0.32 eV, which is quite close to the experimental value of 0.30 eV. We believe that this structure may also be observed; however, it is less stable than **10** (which will be described next) leading us to believe that it probably will not form.

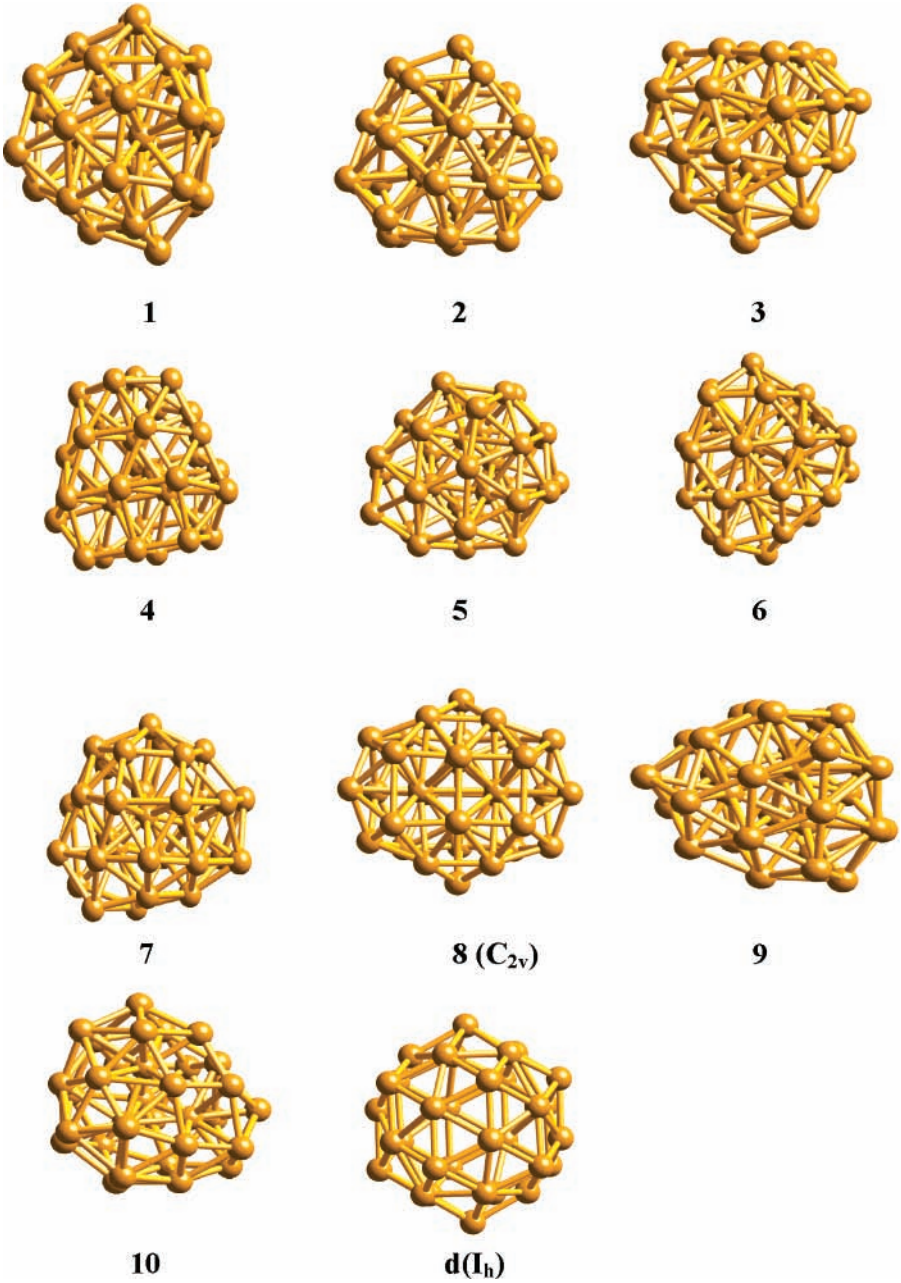

Figure 1. Optimized geometries for the Au_{32} clusters obtained at the DFT level of theory. Except for structures **d** and **8**, all of the other isomers are not symmetric (hence, they belong to the C_1 point group).

TABLE 1: Relative Energies and HOMO−LUMO Gaps in Electronvolts for the Various Isomers Depicted in Figure 1

isomer	GAP	Au_{32}^{+}	Au_{32}	Au_{32}^{-}
d	1.53	0.000	0.000	0.000
1	0.27	0.097	0.289	−0.630
2	0.03	0.161	0.596	−0.330
3	0.24	0.098	0.472	−0.329
4	0.09	0.120	0.579	−0.255
5	0.41	0.347	0.582	−0.194
6	0.24	0.208	0.593	−0.528
7	0.35	0.071	0.267	−0.486
8	0.40	0.356	0.659	−0.201
9	0.32	0.037	0.373	−0.364
10	0.34	−0.016	0.205	−0.672

The final structure that we study is isomer **10**, which is also a low-symmetry (disordered) cluster. As we can see from Table 1, at the DFT level, this isomer is the most stable anion and cation. Additionally, the calculations for the neutral isomer revealed that it is only about 0.21 eV higher in energy than isomer **d**. Therefore, the lowest energy structure we found for Au_{32}^{-} and Au_{32}^{+} clusters is isomer **10**. It is important to note that while we considered over 200 isomers in the initial scan (which was reduced to 11 lowest energy candidates) the scan of the potential energy surface is by no means complete. From Table 1, one can also notice that the HOMO/LUMO gap is around 0.34 eV, which is rather close to the experimental value of 0.30 eV. While isomers **1** and **9** also have a HOMO/LUMO gap in close experimental agreement, the increased stability of **10** leads us to believe that this will be the preferred experimental geometry.

Previous calculations[15] suggest that **d** is in fact the lowest energy structure for the anion, but our calculations indicate that isomer **10** should be. One possible reason for this discrepancy is that, in the previous calculations,[15] a variety of structures that do not possess symmetry in a systematic way were not considered. Rather, in those calculations, only two disordered isomers and four symmetric structures were considered.

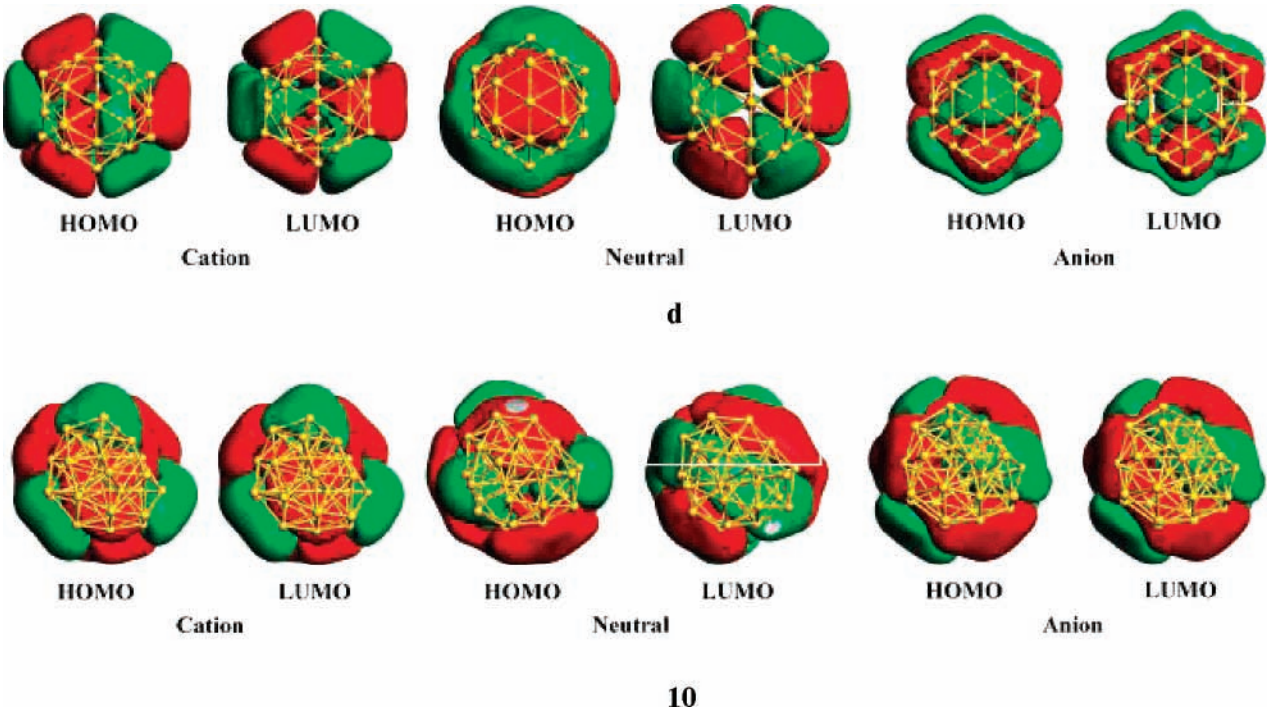

Figure 2. HOMO and LUMO isosurfaces (at the 0.022 au contour level) for species **d** and **10**.

Figure 2 presents HOMO and LUMO representations of the molecular orbitals formed in the neutral, cationic, and anionic states of **d** and **10**, calculated at the DFT level of theory. We only discuss the electron distribution results for these two isomers since our computations suggest that they are the most relevant structures along the potential energy surface.

Also, it is interesting to compare the charge distribution between a cagelike structure (isomer **d**) and a low-symmetry compact structure (isomer **10**). From Figure 2, it is clear that, for the neutral species, both structures have a similar distribution of HOMO electron densities. Once an electron is added or removed, the HOMO in **d** is delocalized along the whole structure similar to a fullerene structure. It is important to at least distinguish that these structures do mediate charge properly as is observed by the HOMO electron distribution. Figure 2 adequately shows how the excess electron is stabilized in both gold cluster isomers. The structures shows very little capability in forming a delocalized system indicative of stable gold clusters as two excess electrons are attached to the complex.[14] Indeed the charge distributions displayed are aimed to better depict the method by which these interesting structures delocalize excess charge. The purpose of the present discussion is to graphically justify the excess electron binding pattern to the Au_{32} molecular surface.

To further emphasize the point being discussed above in relation to the higher stability of **10** over **d** in the charged Au_{32} cluster isomers, we have performed calculations on the dication and dianion states of this cluster. Figure 3 displays the HOMO and LUMO electron density plots for these species. Panels a and b are the dicationic and dianionic forms of **10**, respectively. Panels c and d are the dicationic and dianionic forms of **d**, respectively. Figure 3 shows that, when a second electron is taken away, the cluster structure does not change significantly. However, after addition of a second excess electron, the cluster deforms drastically. Also, it is notorious that, for the dicationic and dianionic states, similar low-symmetry structures are obtained upon relaxation of isomer **10**, but for the **d** isomer, the structure stretches in order for the excess electrons to occupy larger cavities within the cluster volume.

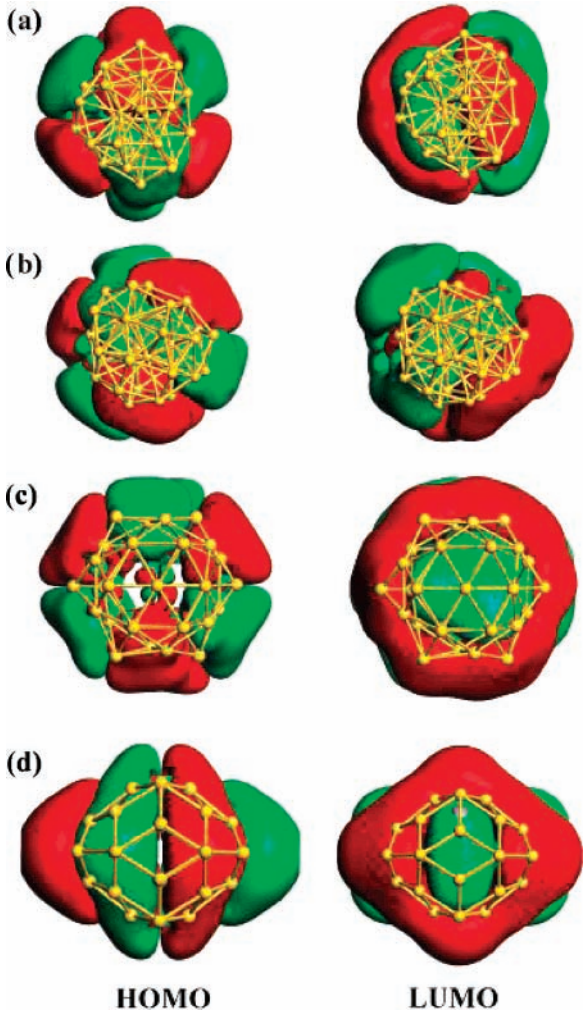

Figure 3. HOMO and LUMO isosurfaces (at the 0.022 au contour level) for the dicationic (Au_{32}^{+2}; a) and the dianionic (Au_{32}^{-2}; b) for isomer **10**, respectively. In c and d, the electron density plots for the dicationic and dianionic forms of isomer **d**, respectively, are displayed.

Conclusions

Overall, we have explored the plausibility that low-symmetry (disordered) isomers of the Au_{32} cluster may have higher energetic stability than the icosahedral cagelike structure. While the symmetric cagelike isomer **d** is more stable in the neutral state, our DFT−GGA calculations have shown that upon electron attachment the low-symmetry (disordered) cluster structures are lower in energy. Upon electron detachment from the neutral cluster, **d** is more stable than several isomers except for isomer **10**, which is also a low-symmetry disordered cluster, although very close in energy to isomer **d**. Other evidence leading to favor isomer **10** over isomer **d**, is the HOMO/LUMO gap of 0.34 eV, as it is compared with the experimental value of 0.30 eV.[15] The low-symmetry (disordered) isomers of the Au_{32}^{-} cluster reported here not only are more stable than the isomer **d** but also appear to be more reactive with lower values of the HOMO/LUMO.

While the above results were obtained using a reliable DFT−GGA−PBE methodology,[11,28] further calculations based on higher levels of theory are expected to get additional insights in the interplay between geometric and electronic structures of neutral and charged Au_{32} cluster isomers, that show changes in their energy ordering by the attachment or detachment of a single electron. Work in that direction is in progress.

In summary, the main contribution of the present calculations, performed at $T = 0$ K, is the prediction that low-symmetry (disordered) isomers should be observed for the anionic Au_{32}^{-} cluster not only at room temperatures, as was already reported,[15] but also at much lower temperatures. Therefore, further experiments are expected at lower temperatures to overcome entropic effects, which may prevent an adequate physical interpretation of the energy landscape of neutral and charged Au_{32} clusters.

Acknowledgment. We thank Dr. Mikael Johansson and Dr. Karo Michaelian for useful discussions at the initial stage of this work and to DGSCA-UNAM for valuable computer resources used in this research. This work was supported by Conacyt-México under Project 43414-F.

Supporting Information Available: Full description of the *x*,*y*,*z* coordinates of the calculated structures presented in the text. This material is available free of charge via the Internet at http://pubs.acs.org.

References and Notes

(1) Mirkin, C. A.; Letsinger, R. L.; Mucic, R. C.; Storhoff, J. *Nature (London*) **1996**, *382*, 607.

(2) Alivisatos, A. P.; Johnsson, K. P.; Peng, X.; Wilson, T. E.; Loweth, C. J.; Bruchez, M. P.; Schultz, P. G. *Nature (London*) **1996**, *382*, 609.

(3) Whetten, R. L.; Khoury, J. T.; Alvarez, M. M.; Murthy, S.; Vezmar, I.; Wang, Z. L.; Stephens, P. W.; Cleveland, C. L.; Luedtke, W. D.; Landman, U. *Adv. Mater*. **1996**, *5*, 8.

(4) Haruta, M. *Catal. Today* **1997**, *36*, 153.

(5) Schwerdtfeger, P. *Angew. Chem., Int. Ed*. **2003**, *42*, 192.

(6) Daniel, M. C.; Astruc, D. *Chem. Rev*. **2004**, *104*, 293.

(7) Meyer, R.; Lemire, C.; Shaikhutdinov, Sh. K.; Freund, H.-J. *Gold Bull. (London*) **2004**, *37*, 72.

(8) Pyykkö, P. *Angew. Chem., Int. Ed*. **2004**, *43*, 4412.

(9) Pyykkö, P. *Inorg. Chim. Acta* **2005**, *358*, 4113.

(10) Xing, X.; Yoon, B.; Landman, U.; Parks, J. H. *Phys. Rev. B* **2006**, *74*, 165423, and references therein.

(11) Fernández, E. M.; Soler, J. M.; Garzón, I. L.; Balbás, L. C. *Phys. Rev. B* **2004**, *70*, 165403.

(12) Johansson, M. P.; Sundholm, D.; Vaara, J. *Angew. Chem., Int. Ed*. **2004**, *43*, 2678.

(13) Gu, X.; Ji, M.; Wei, S. H.; Gong, X. G. *Phys. Rev. B* **2004**, *70*, 205401.

(14) Wang, J. L.; Jellinek, J.; Zhao, J.; Chen, Z. F.; King, R. B.; Schleyer, P. V. *J. Phys. Chem. A* **2005**, *109*, 9265.

(15) Ji, M.; Gu, X.; Li, X.; Gong, X. G.; Li, J.; Wang, L. S. *Angew. Chem., Int. Ed*. **2005**, *44*, 7119.

(16) Xing, X.; Danell, R. M.; Garzón, I. L.; Michaelian, K.; Blom, M. N.; Burns, M. M.; Parks, J. H. *Phys. Rev. B* **2005**, *72*, 081405.

(17) Schooss, D.; Blom, M. N.; Parks, J. H.; v Issendorff, B.; Haberland, H.; Kappes, M. M. *Nano Lett*. **2005**, *5*, 1972.

(18) Blom, M. N.; Schooss, D.; Stairs, J.; Kappes, M. M. *J. Chem. Phys*. **2006**, *124*, 244308.

(19) Lechtken, A.; Schooss, D.; Stairs, J. R.; Blom, M. N.; Furche, F.; Morgner, N.; Kostko, O.; v. Issendorff, B.; Kappes, M. M. *Angew. Chem., Int. Ed*. **2007**, *46*, 2944.

(20) Li, J.; Li, X.; Zhai, H. J.; Wang, L. S. *Science* **2003**, *299*, 864.

(21) Bulusu, S.; Li, X.; Wang, L. S.; Zeng, X. C. *J. Phys. Chem. C* **2007**, *111*, 4190, and references therein.

(22) Garzón, I. L.; Michaelian, K.; Beltrán, M. R.; Posada-Amarillas, A.; Ordejón, P.; Artacho, E.; Sánchez-Portal, D.; Soler, J. M. *Phys. Rev. Lett*. **1998**, *81*, 1600.

(23) Garzón, I. L.; Reyes-Nava, J. A.; Rodríguez-Hernández, J. I.; Sigal, I.; Beltrán, M. R.; Michaelian, K. *Phys. Rev. B* **2002**, *66*, 073403.

(24) Lopez-Lozano, X.; Pérez, L. A.; Garzón, I. L. *Phys. Rev. Lett*. **2006**, *97*, 233401, and references therein.

(25) Soler, J. M.; Artacho, E.; Gale, J. D.; García, A.; Junquera, J.; Ordejón, P.; Sánchez-Portal, D. *J. Phys. Condens. Matter* **2002**, *14*, 2745.

(26) Troullier, N.; Martins, J. L. *Phys. Rev. B* **1991**, *43*, 1993.

(27) Perdew, P.; Burke, K.; Ernzerhof, M. *Phys. Rev. Lett.* **1996**, *77*, 3865.

(28) Fernández, E. M.; Soler, J. M.; Balbás, L. C. *Phys. Rev. B* **2006**, *73* 235433.